Application of M3D-C^1 to Studying 2-Fluid Magnetic Reconnection in the Presence of a Guide Field

S. C. Jardin, N. Ferraro, J. Breslau
Princeton Plasma Physics Laboratory

CEMM Meeting
Sherwood Conference, Boulder, CO
March 30, 2008

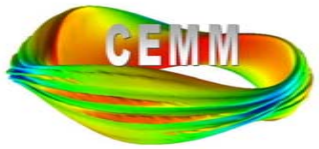

Outline:

- 2F magnetic reconnection without guide field – GEM (review)
- 2F magnetic reconnection with guide field

-- if time permits –

- M3D-C^1 development update
  - New developments in formalism of M3D-C^1 (& NIMROD) time advance
  - Adaptive Zoning
  - Status and Plans

“GEM” reconnection test problem[1] for 2-fluid MHD

In-plane current density contours at different times

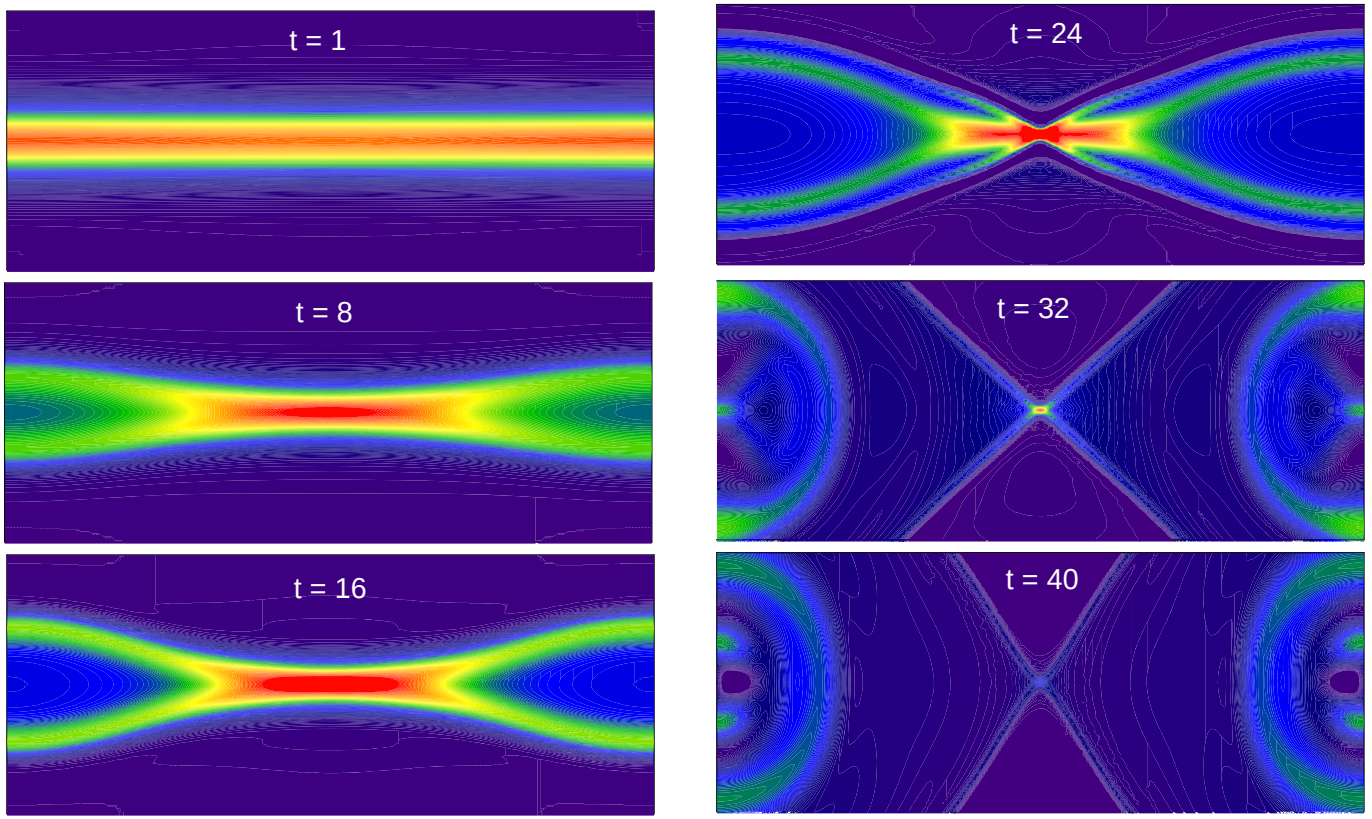

- Starts like resistive MHD
- Dramatic change in configuration for t > 20

[1]J. Birn, et al, J. Geophys. Res. 106 (2001) 3715

2-fluid reconnection requires high resolution for convergent results

- Note sudden transition where velocity abruptly increases
- These calculations used a hyperviscosity term in Ohm's law proportional to $(\Delta x)^2 \cdots$ required for a stable calculation
- Reconnected Flux at t=40 converges as $1/h^5$

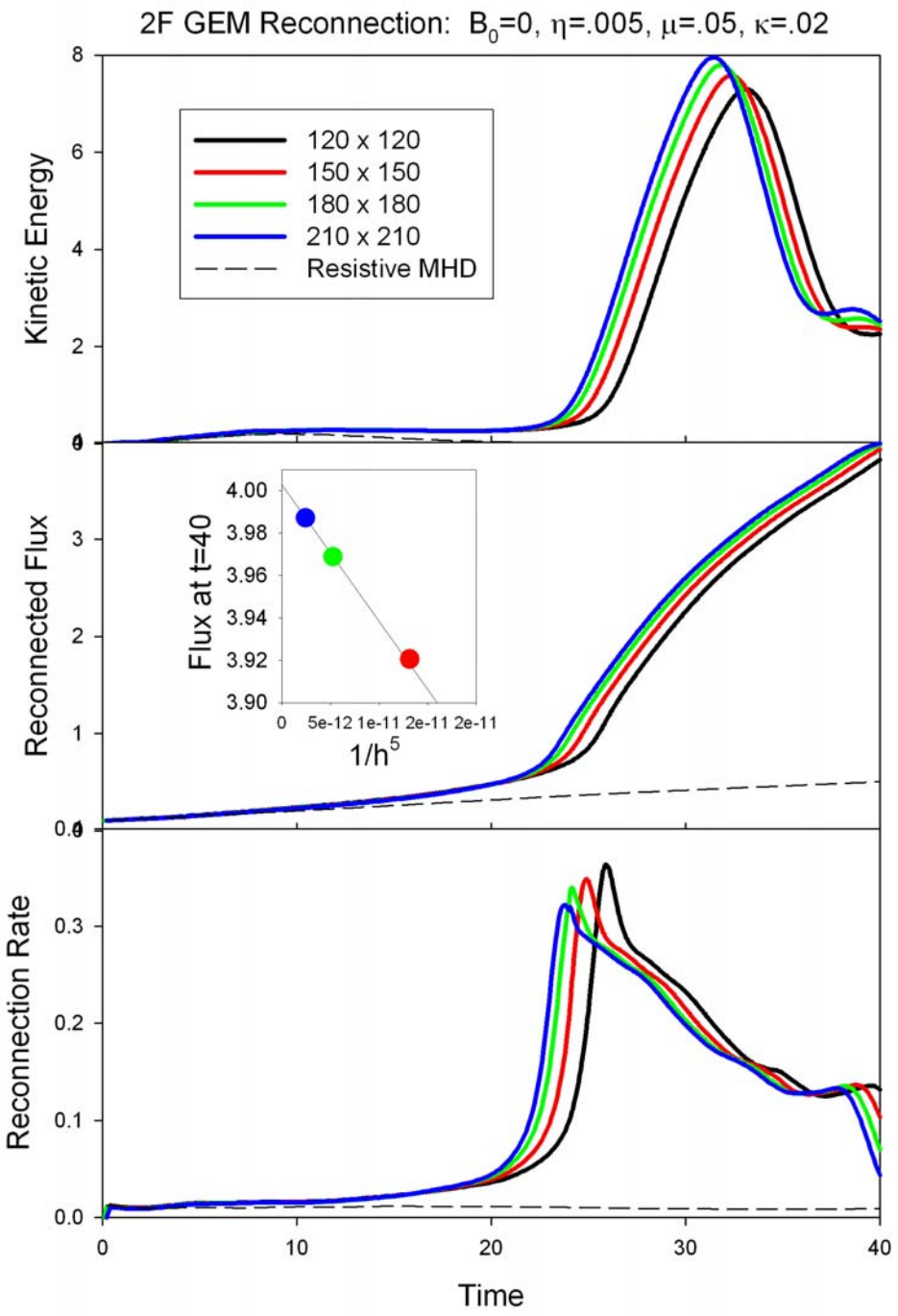

2F GEM Reconnection snapshot at time of maximum velocity t ~ 32 (200^2 nodes)

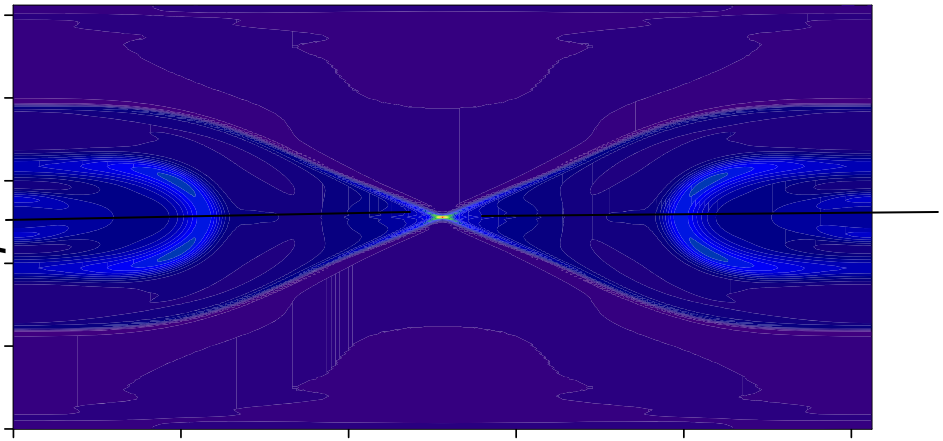

out-of-plane current

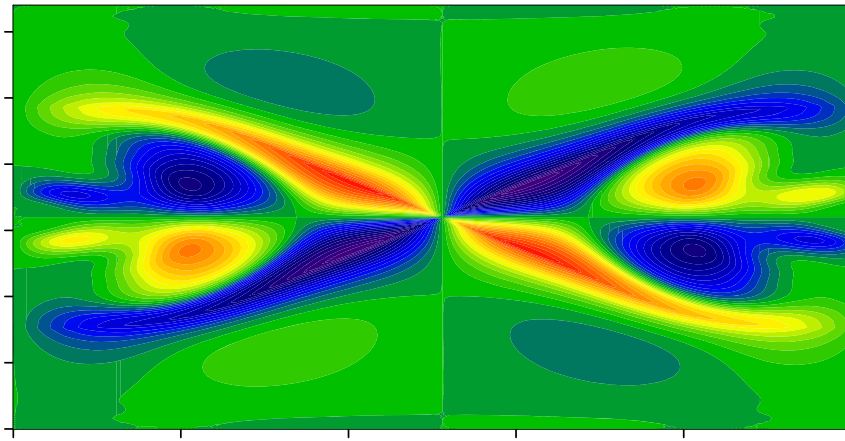

out-of-plane magnetic field

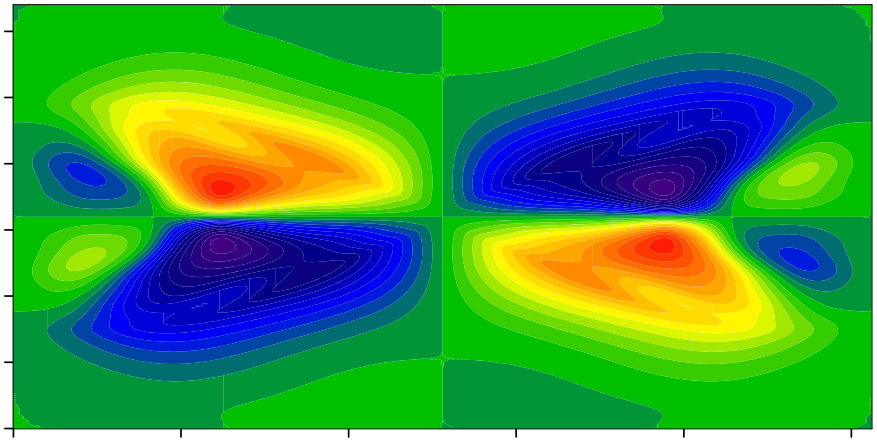

vorticity field

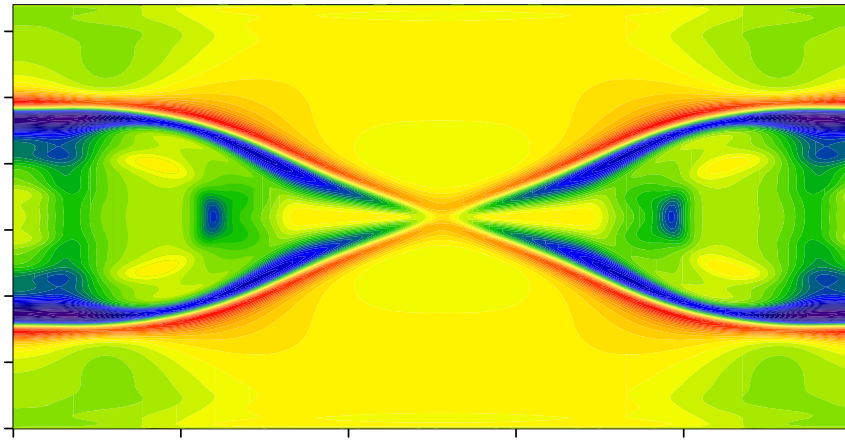

velocity divergence

Energy conservation to 1 in 10^3, flux conservation exact, symmetry preserved even though triangles were not arranged symmetrically.

Midplane Current density collapses to the width of 1-3 triangular elements

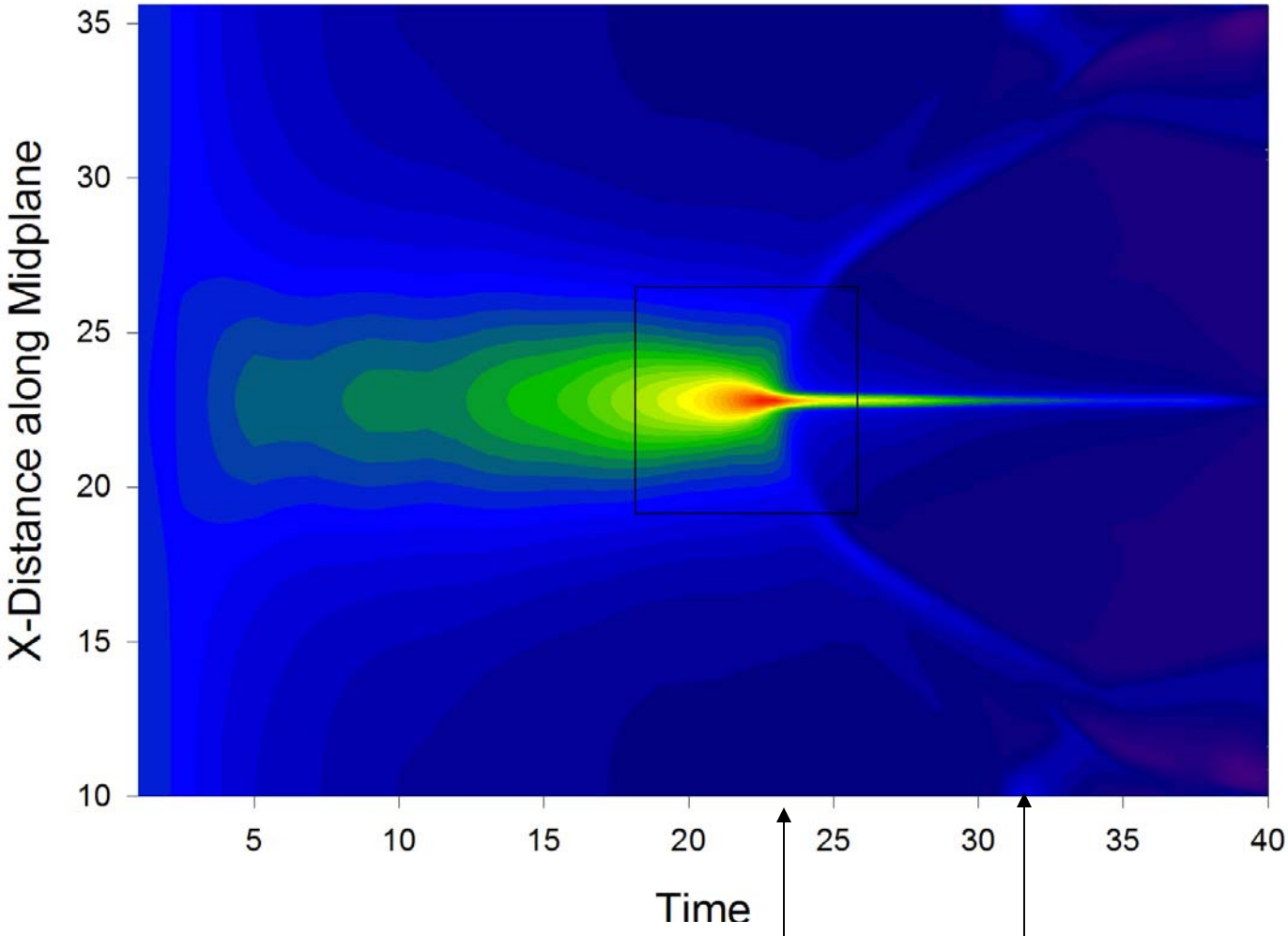

Midplane electric field before and after transition

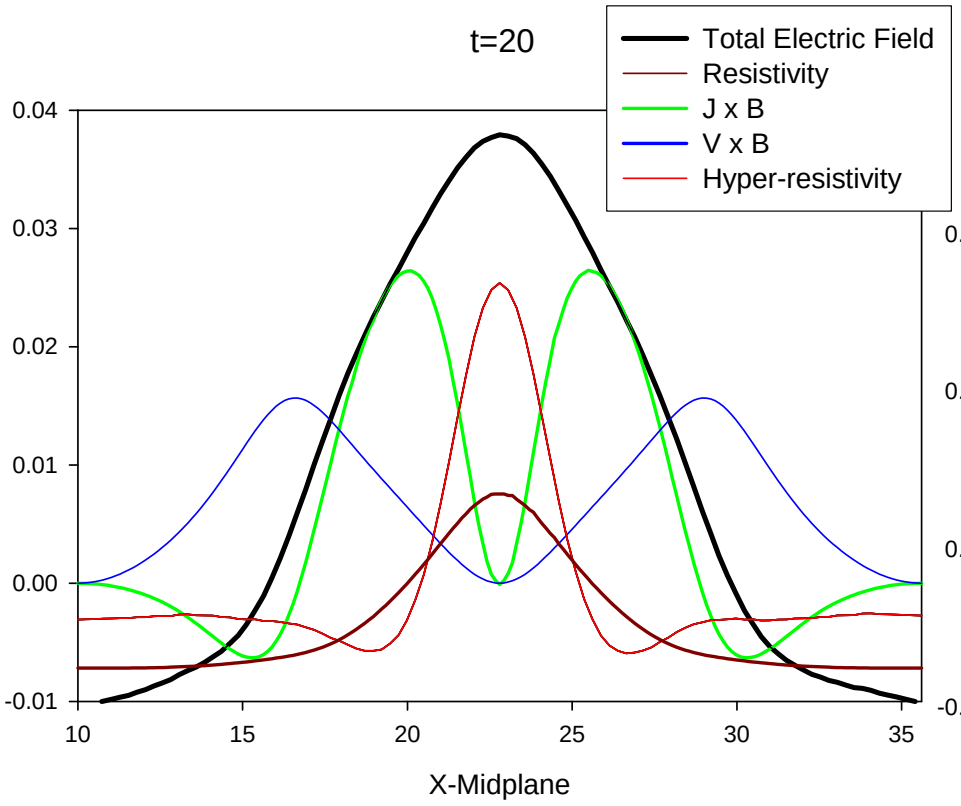

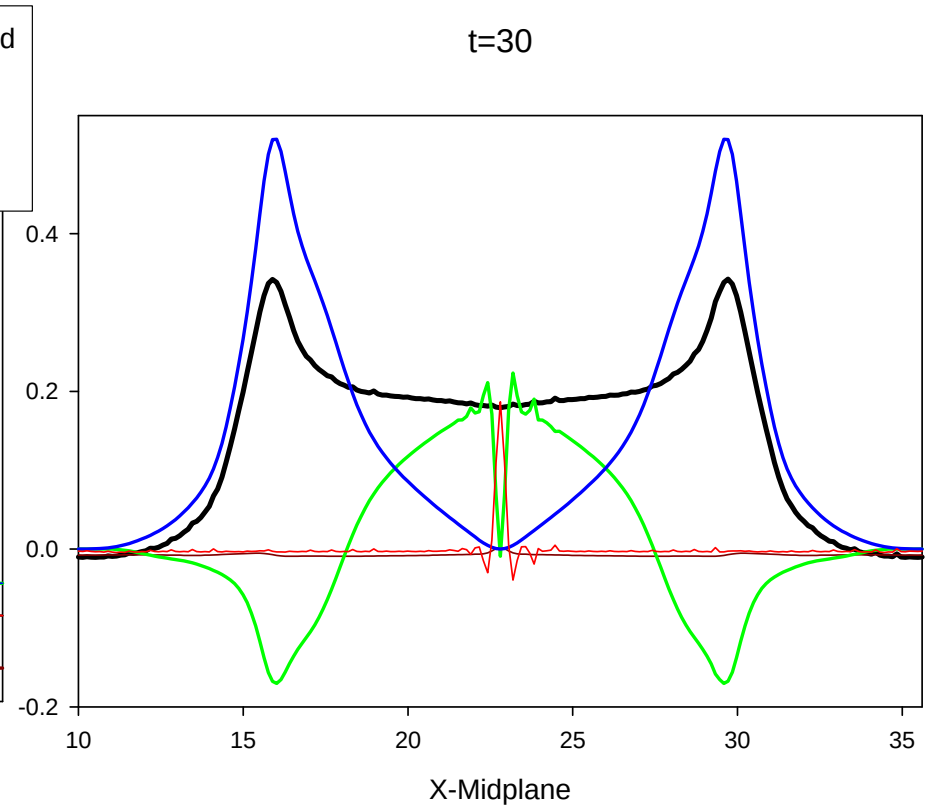

Reconnection rate: $\hat{z}\bullet\left[\vec{E}=-\vec{V}\times\vec{B}+\eta\vec{J}+\frac{1}{ne}\left(\vec{J}\times\vec{B}-\nabla p_e\right)-\lambda_H(\Delta x)^2\nabla^2\vec{J}\right]$

Blowup showing electric field after transition

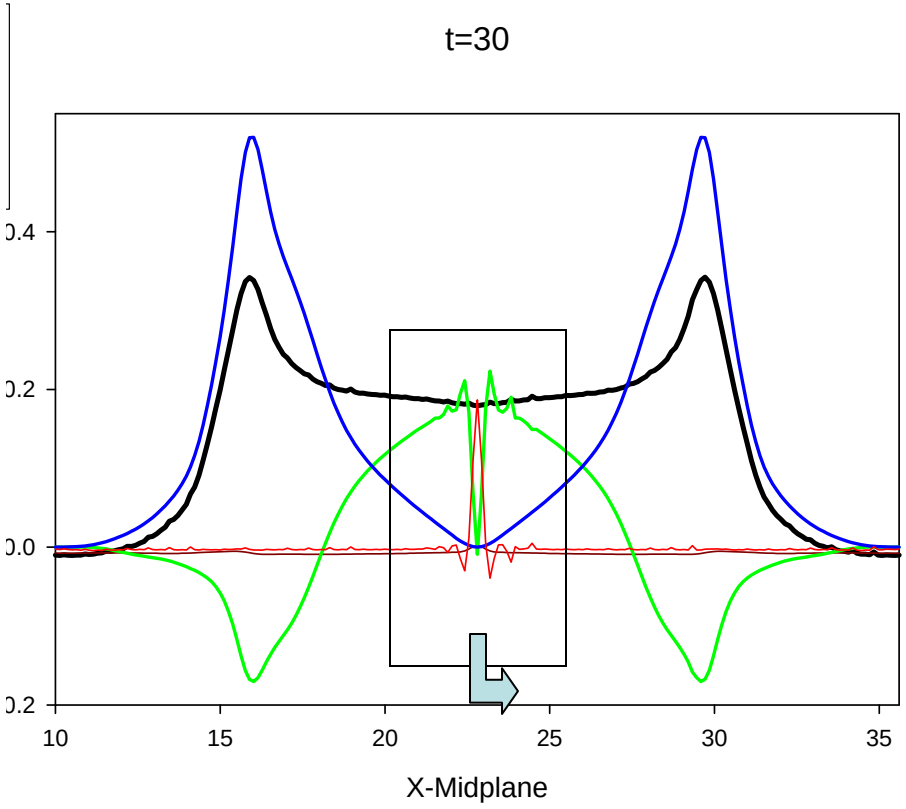

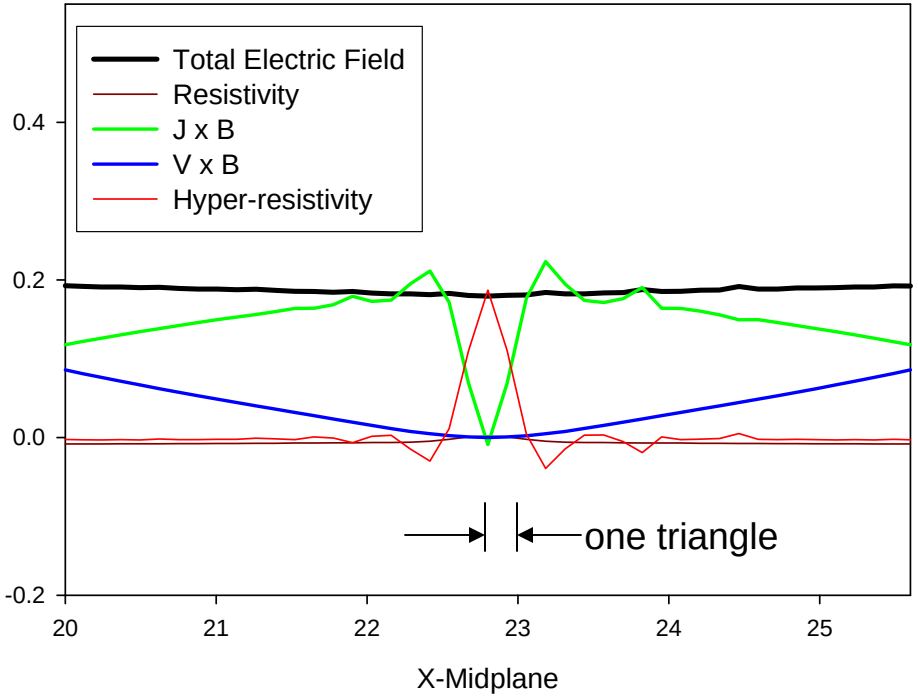

$$\hat{z}\bullet\left[\vec{E}=-\vec{V}\times\vec{B}+\eta\vec{J}+\frac{1}{ne}\left(\vec{J}\times\vec{B}-\nabla p_e\right)-\lambda_H(\Delta x)^2\nabla^2\vec{J}\right]$$

Hyper-resistivity coefficient must be large enough that current density collapse is limited to 1-2 triangles: *reason for factor* $(\Delta x)^2$8

2F GEM reconnection with Guide Field

Calculations were repeated with a magnetic field B_0 in the direction of the symmetry (guide field). This better approximates reconnection in a tokamak.

We find that the reconnection rate is dramatically reduced as B_0 is increased.

Part of this effect is because the B_0 inhibits density depletion, which was accelerating the reconnection in the standard GEM case with B_0=0.

$$\mathbf{E}+\mathbf{V}\times\mathbf{B}=\eta\mathbf{J}+\frac{d_i}{ne}\left(\mathbf{J}\times\mathbf{B}-\nabla p_e\right)-\lambda_H\nabla^2\mathbf{J}$$

Ion skin depth increases as density depletes, thus making 2F effects more pronounced.

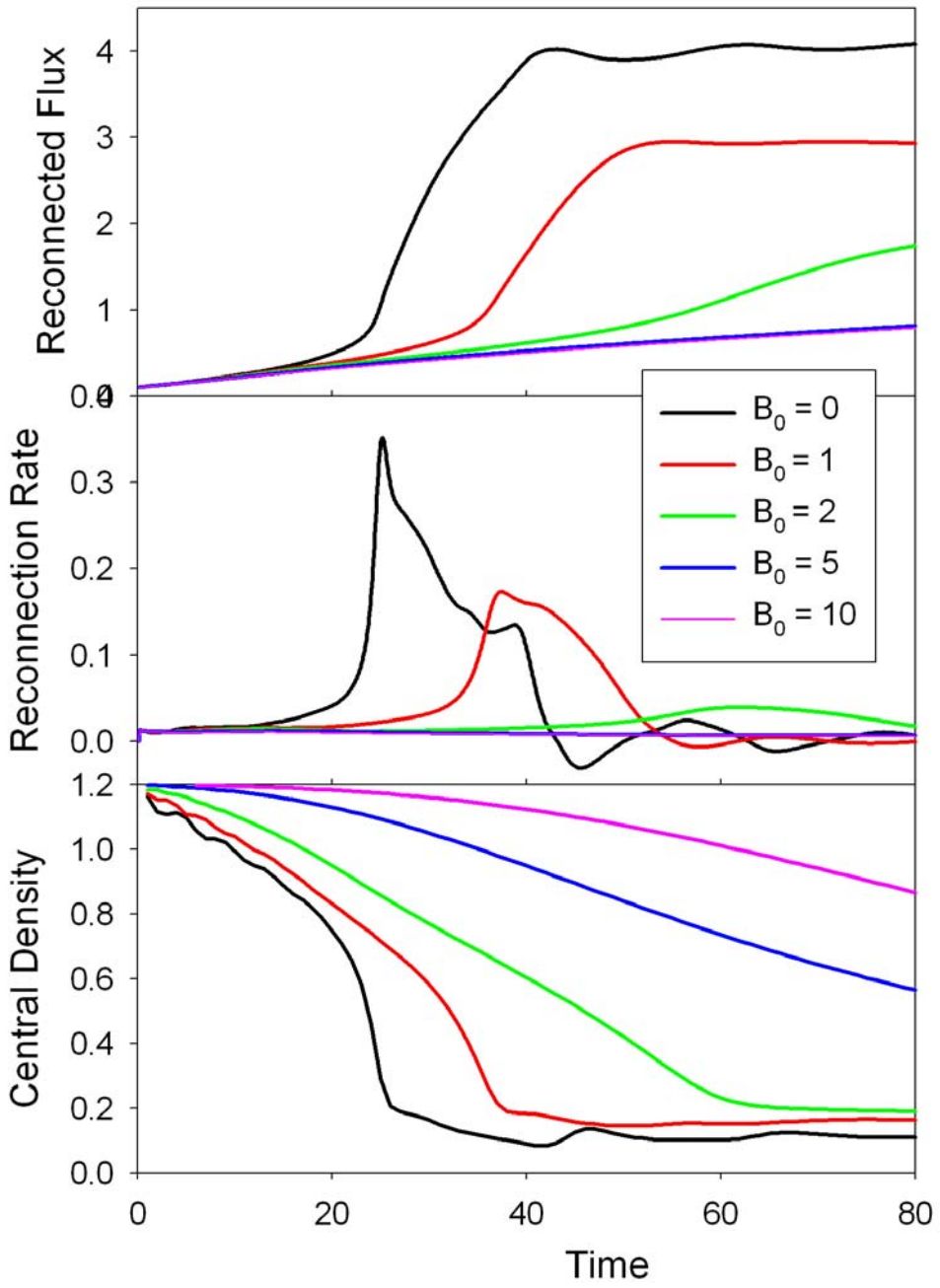

2F GEM reconnection with Guide Field (cont)

To separate the effect of the guide field and the density depletion, we redid the calculations artificially keeping the density fixed at it's initial value.

We find that the reconnection rate is still reduced as B_0 is increased, but not as dramatically.

Note that the d_i parameter was increased from the nominal value of 1 to 5 to see any effect.

$$\mathbf{E}+\mathbf{V}\times\mathbf{B}=\eta\mathbf{J}+\frac{d_i}{n_0 e}\left(\mathbf{J}\times\mathbf{B}-\nabla p_e\right)-\lambda_H\nabla^2\mathbf{J}$$

Density was held constant and d_i was increased from 1 to 5 for this series.

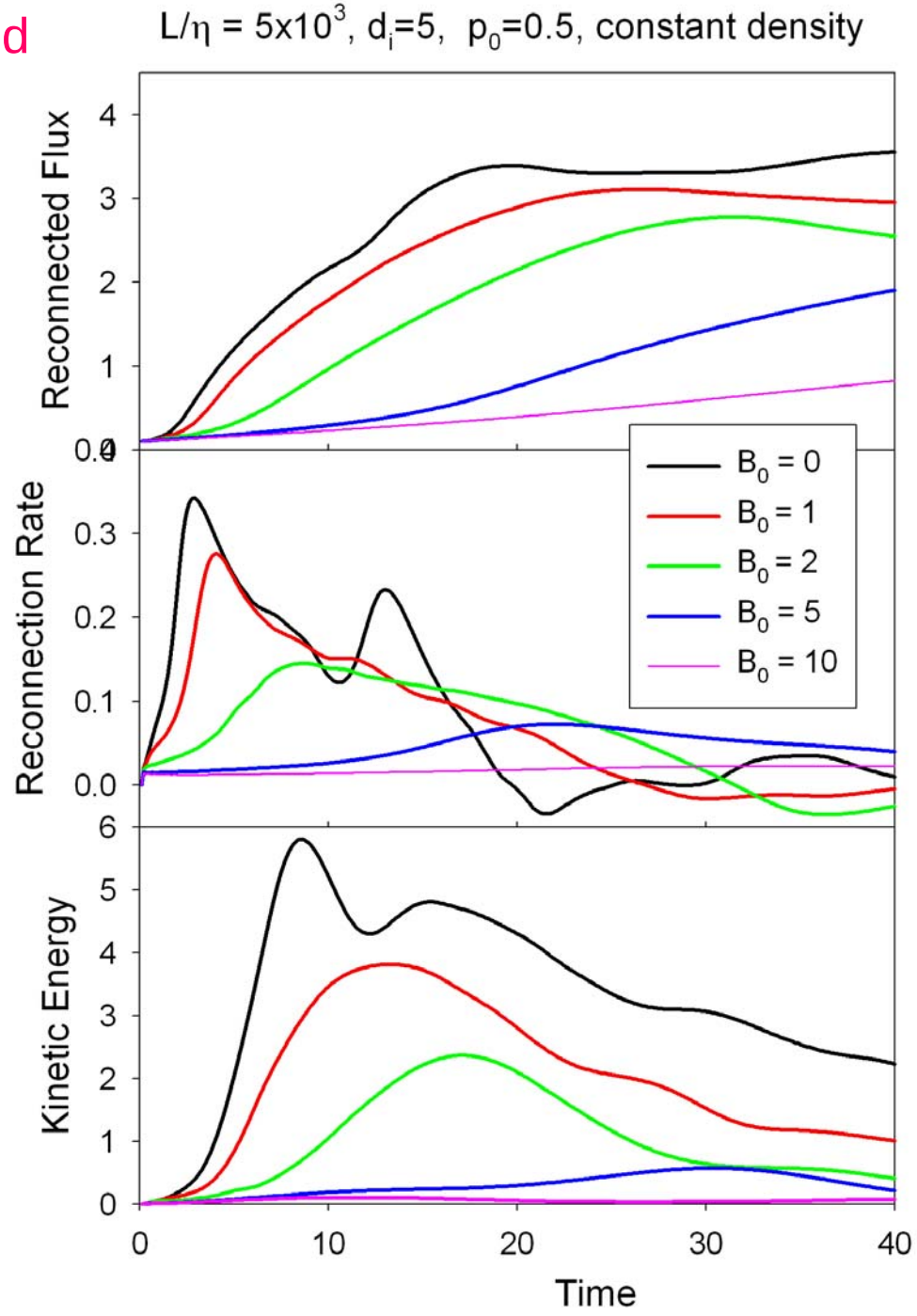

Midplane Electric Field plots at time of maximum reconnection show some similarity, but are reduced by ~ 10 in magnitude.

$B_0 = 0$

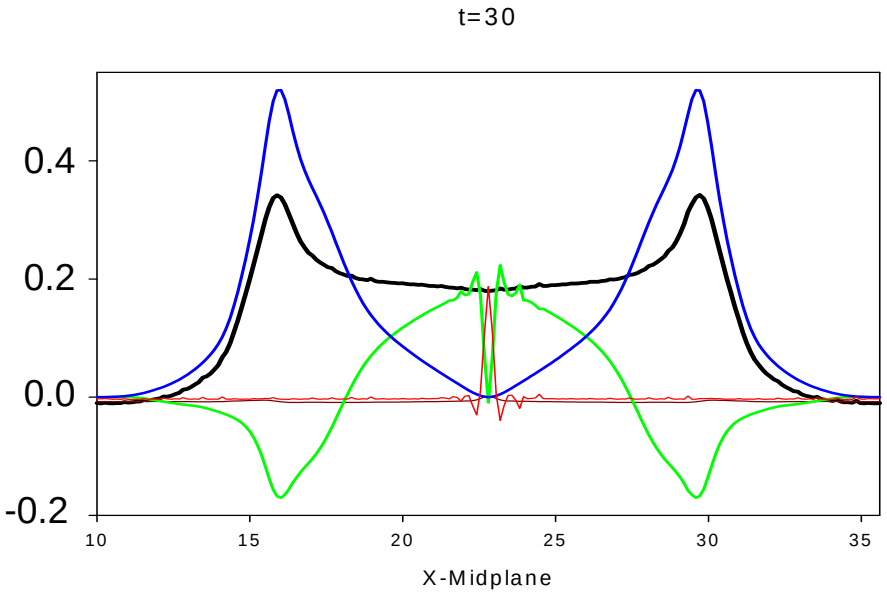

$B_0 = 2$

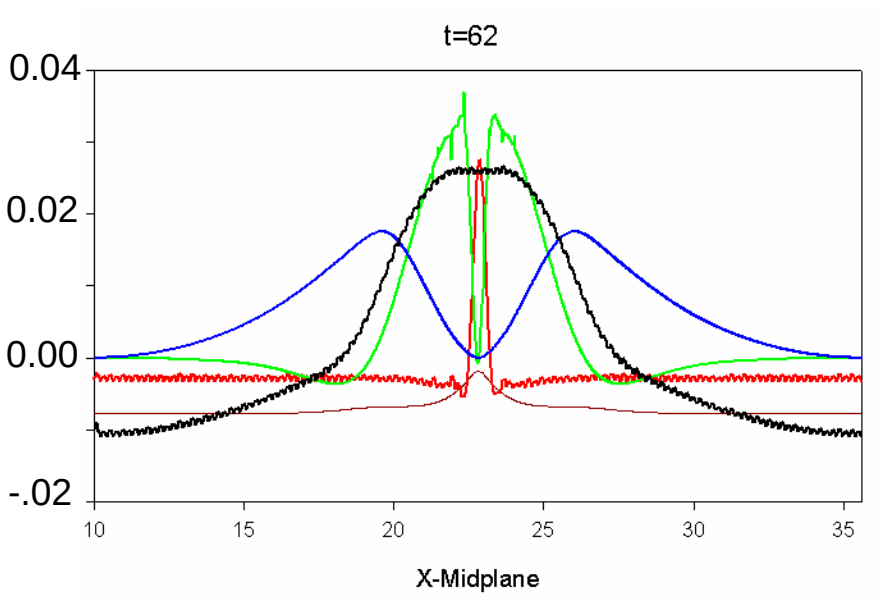

JxB contribution to reconnection electric field much less for guide field case

$B_0 = 0$

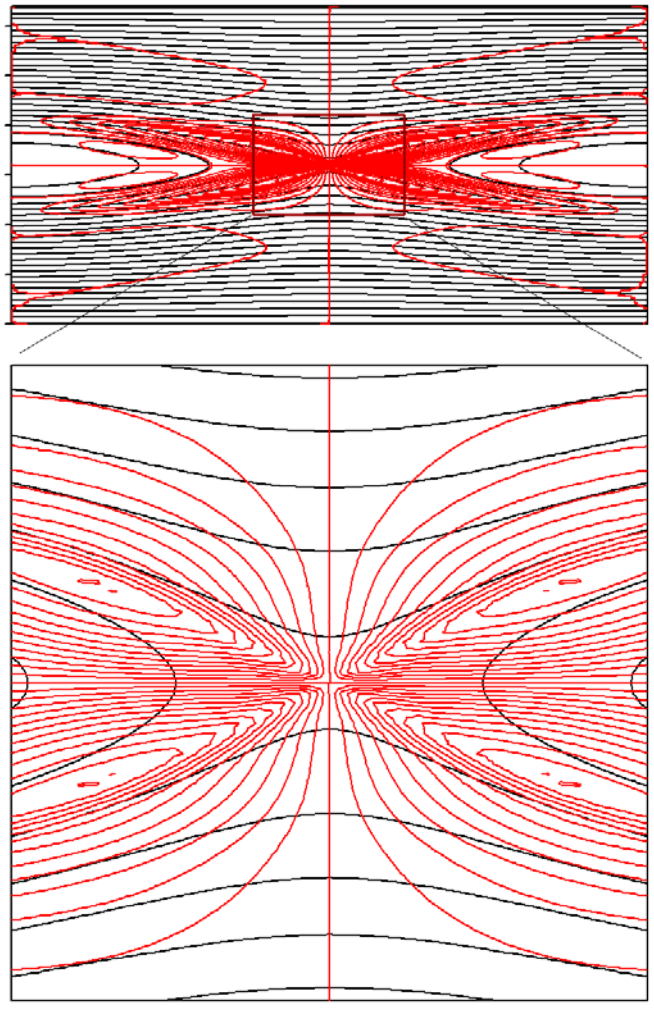

$B_0 = 2$

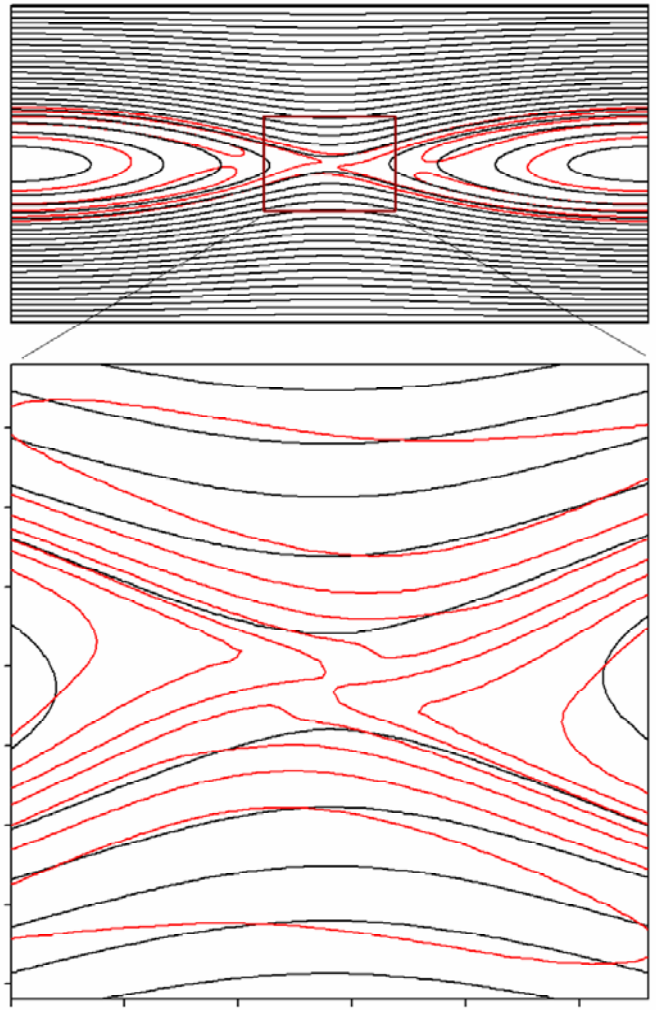

Dark is poloidal field streamlines

Red is poloidal current streamlines

Both ion and electron in-plane velocities greatly reduced with guide field

$B_0 = 0$

$B_0 = 2$

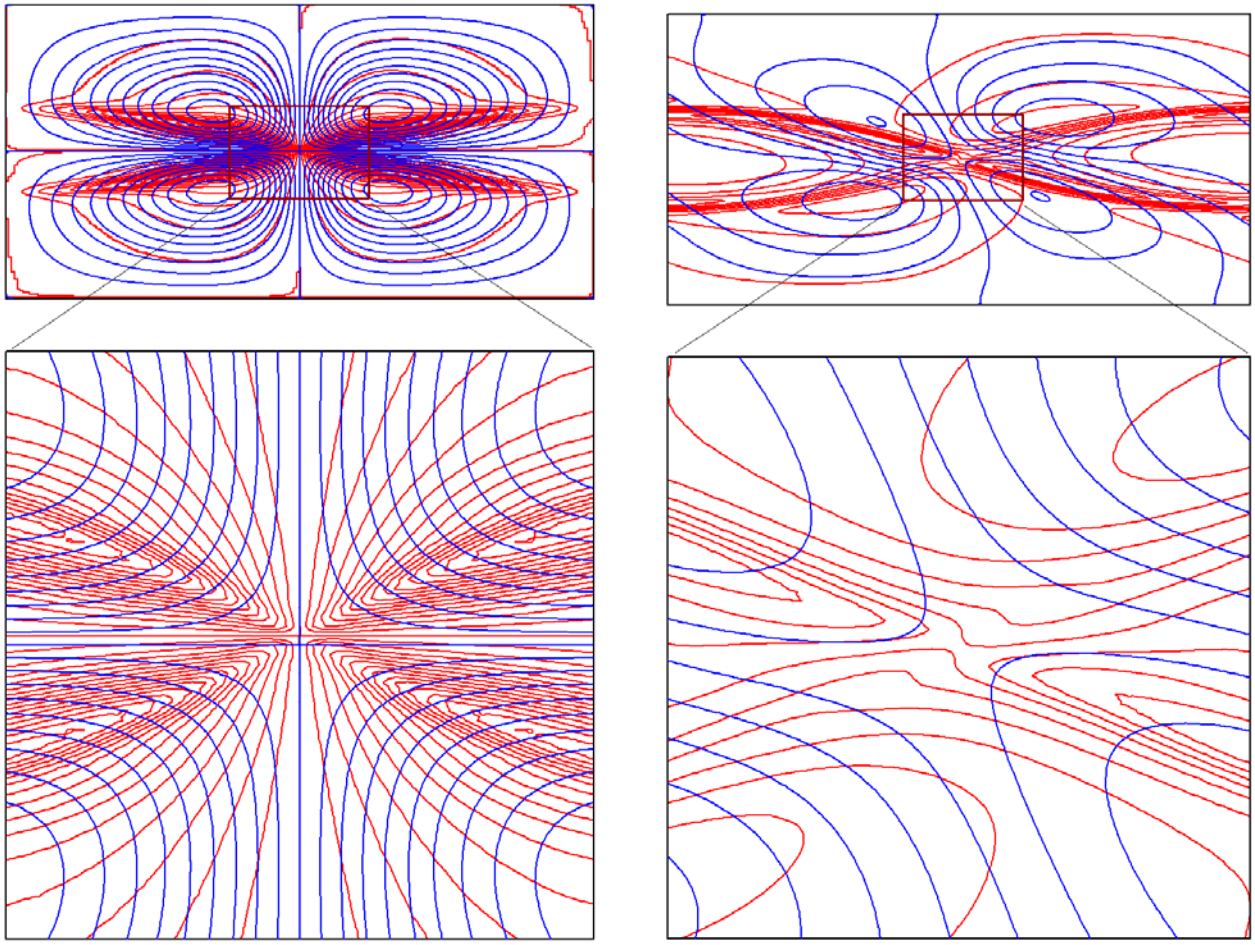

Blue are ion velocity streamlines

Red is electron velocity streamlines

Note: 4-way symmetry replaced by symmetrical twisting

2F GEM reconnection with Guide Field (cont)

We then ran a large number of calculations varying B_0, p_0, d_i, η, ν and performed a regression analysis to find the dependence on these parameters of the peak reconnection rate.

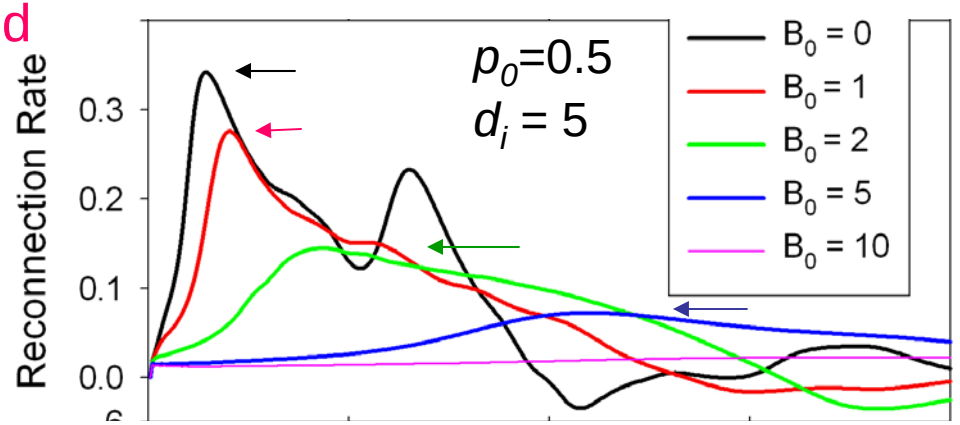

$$\dot{\psi}_{MAX} = C\left[\frac{\beta}{1+\beta}\right]^{A} d_i^{B}\nu^{C}\eta^{D}$$

$\beta = \Gamma p_0 / B_0^2$ $\quad A = .95$

$d_i = c/\omega_{pi}$ $\quad B = .45$

$\nu =$ viscosity $\quad C = -.33$

$\eta =$ resistivity $\quad D = .05$

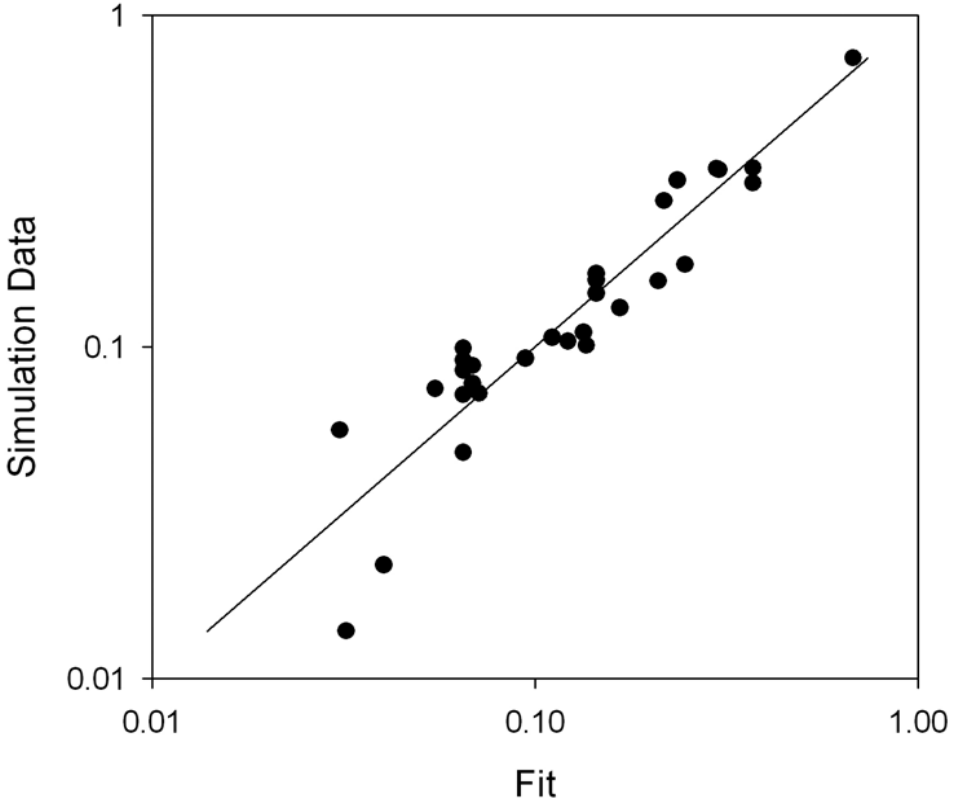

Peak reconnection rate independent of η (resistivity)! This implies that 2F very high S calculations do not require extreme resolution.

Velocity field changes to mostly incompressible as guide field strength is increased

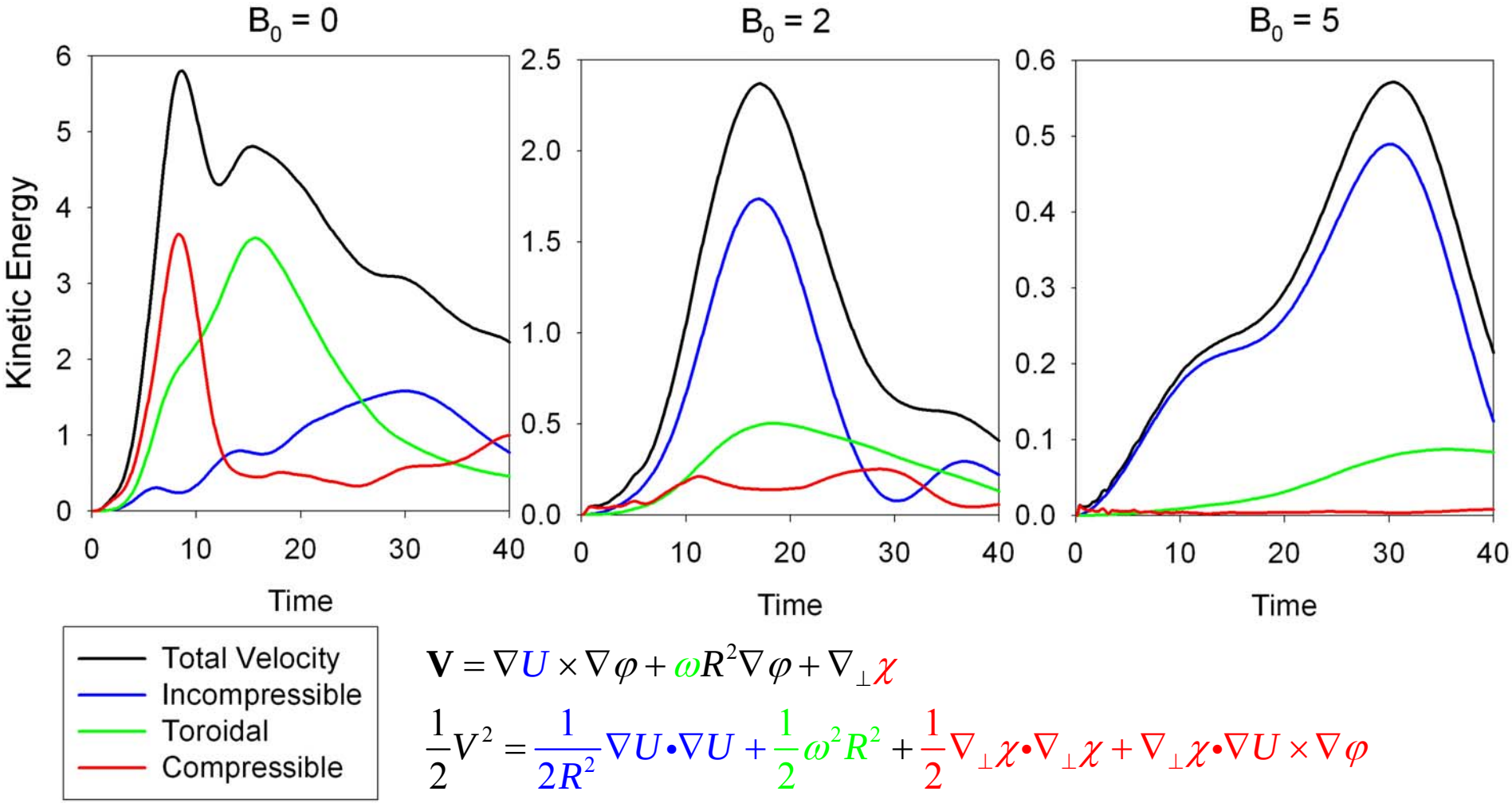

$$\mathbf{V} = \nabla U \times \nabla \varphi + \omega R^2 \nabla \varphi + \nabla_\perp \chi$$

$$\frac{1}{2}V^2 = \frac{1}{2R^2}\nabla U \bullet \nabla U + \frac{1}{2}\omega^2 R^2 + \frac{1}{2}\nabla_\perp \chi \bullet \nabla_\perp \chi + \nabla_\perp \chi \bullet \nabla U \times \nabla \varphi$$

Comparison with 4-variable 2F reduced MHD[1]

Results are in good agreement for $B_0 >> 1$

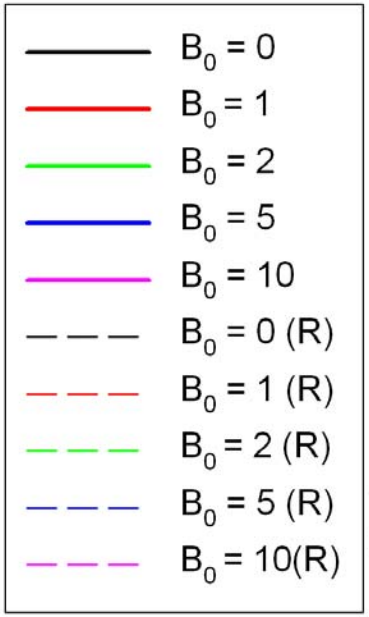

$$\frac{\partial \psi}{\partial t} = [\phi, \psi] + d_i [\psi, B_Z] + \eta \nabla^2 \psi$$

$$\frac{\partial B_Z}{\partial t} = [\phi, B_Z] + c_\beta^2 d_i [\nabla^2 \psi, \psi] + c_\beta^2 [V_z, \psi]$$

$$\frac{\partial \nabla^2 \phi}{\partial t} = [\phi, \nabla^2 \phi] + [\nabla^2 \psi, \psi] + \mu \nabla^4 \phi$$

$$\frac{\partial V_z}{\partial t} = [\phi, V_z] + [B_Z, \psi] + \mu \nabla^2 V_Z$$

$$c_\beta = \sqrt{\beta / (1+\beta)}$$

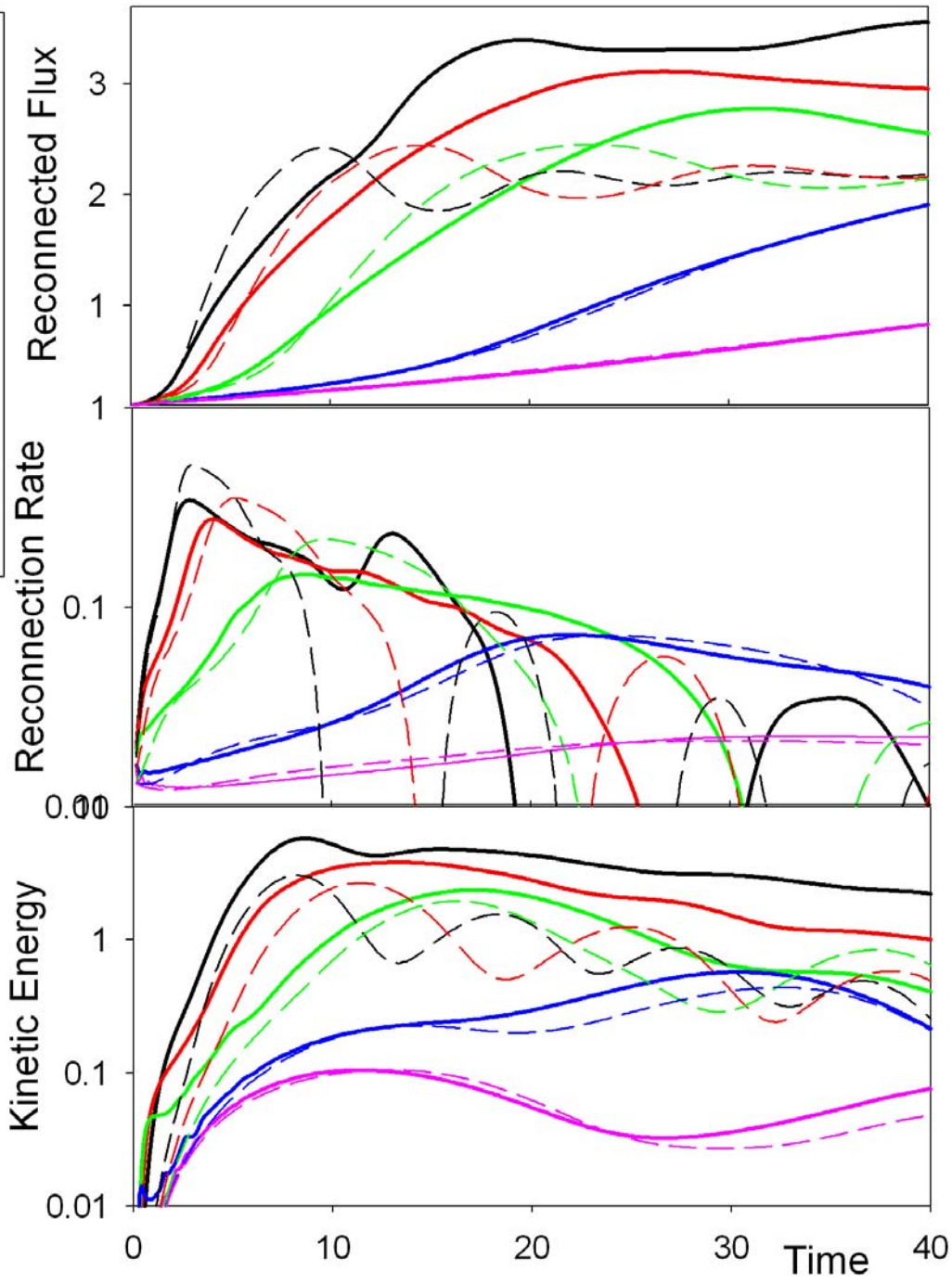

[1]*Fitzpatrick, Phys. Plasmas, **11** 3961 (2004)*

Split Implicit Time Advance applied to the basic 3D MHD equations:

$$\rho_0 \dot{\mathbf{V}} = \frac{1}{\mu_0}\left[\nabla \times \mathbf{B}\right] \times \mathbf{B} - \nabla p$$
$$\dot{\mathbf{B}} = \nabla \times \left[\mathbf{V} \times \mathbf{B}\right]$$
$$\dot{p} = -\mathbf{V} \bullet \nabla p - \gamma p \nabla \bullet \mathbf{V}$$

Ideal MHD Equations for velocity, magnetic field, and pressure:

Symmetric Hyperbolic System

7-waves

$$\rho_0 \dot{\mathbf{V}} = \frac{1}{\mu_0}\left[\nabla \times \left(\mathbf{B} + \theta \delta t \dot{\mathbf{B}}\right)\right] \times \left(\mathbf{B} + \theta \delta t \dot{\mathbf{B}}\right) - \nabla\left(p + \theta \delta t \dot{p}\right)$$
$$\dot{\mathbf{B}} = \nabla \times \left[\left(\mathbf{V} + \theta \delta t \dot{\mathbf{V}}\right) \times \mathbf{B}\right]$$
$$\dot{p} = -\left(\mathbf{V} + \theta \delta t \dot{\mathbf{V}}\right) \bullet \nabla p - \gamma p \nabla \bullet \left(\mathbf{V} + \theta \delta t \dot{\mathbf{V}}\right)$$

Taylor Expand in Time

Substitute from 2nd and 3rd equation into first, finite difference in time:

$$\left\{\rho - \theta^2 (\delta t)^2 L\right\} \mathbf{V}^{n+1} = \left\{\rho - \theta^2 (\delta t)^2 L\right\} \mathbf{V}^{n} + \delta t \left\{-\nabla p + \frac{1}{\mu_0}(\nabla \times \mathbf{B}) \times \mathbf{B}\right\}^{n+1/2}$$

MHD Operator: $\longrightarrow$

$$L\{\mathbf{V}\} = \frac{1}{\mu_0}\left\{\nabla \times \left[\nabla \times \left(\mathbf{V} \times \mathbf{B}\right)\right]\right\} \times \mathbf{B} + \frac{1}{\mu_0}\left(\nabla \times \mathbf{B}\right) \times \left[\nabla \times \left(\mathbf{V} \times \mathbf{B}\right)\right] + \nabla\left(\mathbf{V} \bullet \nabla p + \gamma p \nabla \bullet \mathbf{V}\right)$$

$$L\{\mathbf{V}\} = \frac{1}{\mu_0}\left\{\nabla\times\left[\nabla\times\left(\mathbf{V}\times\mathbf{B}\right)\right]\right\}\times\mathbf{B} + \frac{1}{\mu_0}\left(\nabla\times\mathbf{B}\right)\times\left[\nabla\times\left(\mathbf{V}\times\mathbf{B}\right)\right] + \nabla\left(\mathbf{V}\bullet\nabla p + \gamma p\nabla\bullet\mathbf{V}\right)$$

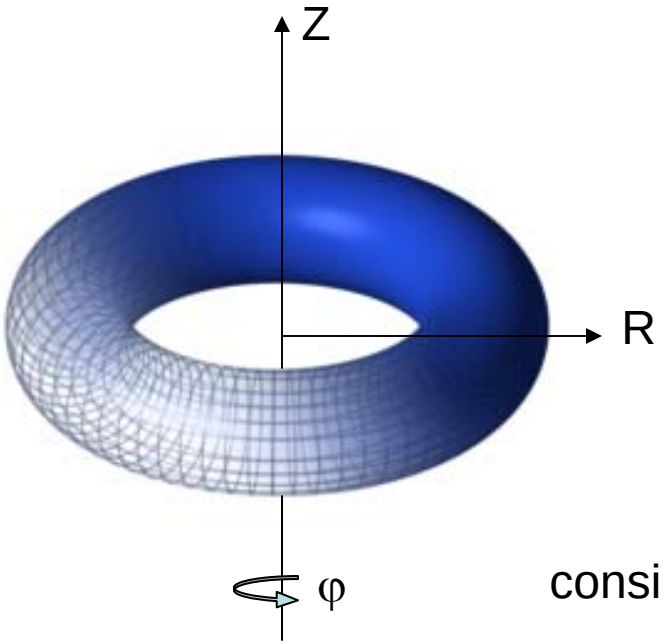

This is the ideal MHD operator of Bernstein, Freeman, Kruskal, and Kulsrud (1958)

Define now 2 displacement (velocity) fields:

$$\mathbf{V} = \nabla U\times\nabla\varphi + \omega R^2\nabla\varphi + \nabla_\perp\chi$$

$$\tilde{\mathbf{V}} = \nabla\tilde{U}\times\nabla\varphi + \tilde{\omega}R^2\nabla\varphi + \nabla_\perp\tilde{\chi}$$

consider the functional:

$$\delta W(\tilde{\mathbf{V}},\mathbf{V}) \equiv \iint d^2R\;\tilde{\mathbf{V}}\bullet L(\mathbf{V})$$

can be broken up into these 9 parts, each of which is a quadratic functional →

$$\begin{aligned}&= \delta W_{11}(\tilde{U},U) + \delta W_{12}(\tilde{U},\omega) + \delta W_{13}(\tilde{U},\chi)\\ &+\delta W_{21}(\tilde{\omega},U) + \delta W_{22}(\tilde{\omega},\omega) + \delta W_{23}(\tilde{\omega},\chi)\\ &+\delta W_{31}(\tilde{\chi},U) + \delta W_{32}(\tilde{\chi},\omega) + \delta W_{33}(\tilde{\chi},\chi)\end{aligned}$$

$$\left\{\rho-\theta^2(\delta t)^2 L\right\}\mathbf{V}^{n+1}=\left\{\rho-\theta^2(\delta t)^2 L\right\}\mathbf{V}^{n}+\delta t\left\{-\nabla p+\frac{1}{\mu_0}(\nabla\times\mathbf{B})\times\mathbf{B}\right\}^{n+1/2}$$

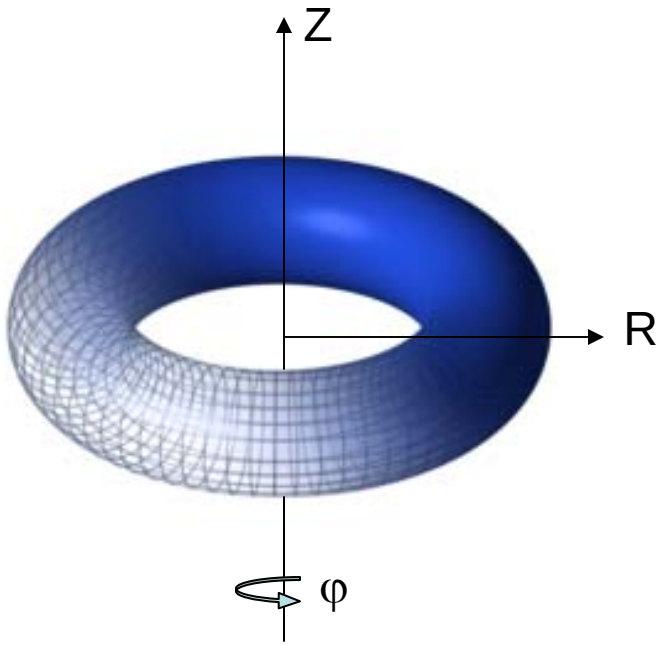

• To solve this by the finite element method, we need to take projections to get scalar equations, and then to take the weak form of those equations.

$$\mathbf{V}=\nabla U\times\nabla\varphi+\omega R^2\nabla\varphi+\nabla_\perp\chi$$

$\nu_i(R,Z)$ is ith finite element trial function

$$-\iint d^2R\,\nu_i\nabla\varphi\bullet\nabla_\perp\times$$
$$\iint d^2R\,\nu_i R^2\nabla\varphi\bullet$$
$$-\iint d^2R\,\nu_i\nabla_\perp\bullet$$

by parts

$$\iint d^2R\,\nabla_\perp\nu_i\times\nabla\varphi\bullet$$
$$\iint d^2R\,\nu_i R^2\nabla\varphi\bullet$$
$$\iint d^2R\,\nabla_\perp\nu_i\bullet$$

Projection or annihilation operators:

Same form as velocity!

$$\left\{\rho-\theta^2(\delta t)^2 L\right\}\mathbf{V}^{n+1}=\left\{\rho-\theta^2(\delta t)^2 L\right\}\mathbf{V}^{n}+\delta t\left\{-\nabla p+\frac{1}{\mu_0}(\nabla\times\mathbf{B})\times\mathbf{B}\right\}^{n+1/2}$$

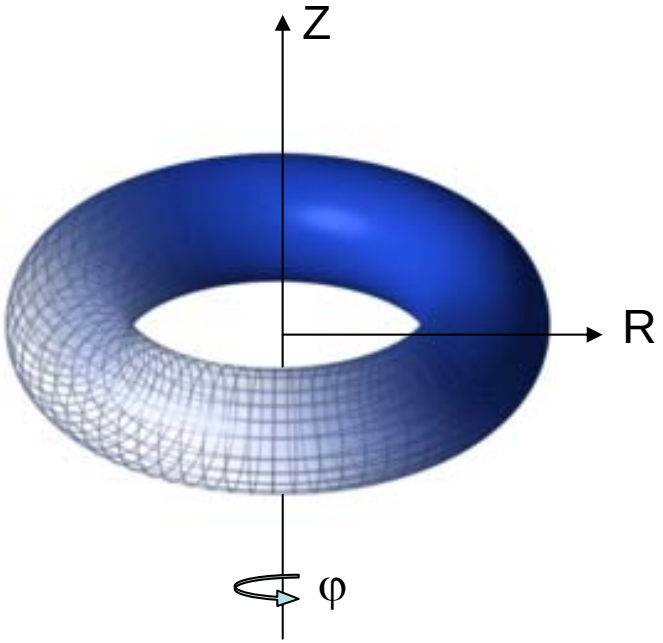

• Consider the effect of these projection operators on the MHD operator

$$L\{\mathbf{V}\}=\frac{1}{\mu_0}\left\{\nabla\times\left[\nabla\times\left(\mathbf{V}\times\mathbf{B}\right)\right]\right\}\times\mathbf{B}$$
$$+\frac{1}{\mu_0}\left(\nabla\times\mathbf{B}\right)\times\left[\nabla\times\left(\mathbf{V}\times\mathbf{B}\right)\right]+\nabla\left(\mathbf{V}\bullet\nabla p+\gamma p\nabla\bullet\mathbf{V}\right)$$

$$\mathbf{V}=\nabla U\times\nabla\varphi+\omega R^2\nabla\varphi+\nabla_\perp\chi$$

$$\iint d^2R\,\nabla_\perp\nu_i\times\nabla\varphi\bullet L\{\mathbf{V}\}$$
$$\iint d^2R\,\nu_i R^2\nabla\varphi\bullet L\{\mathbf{V}\}\longrightarrow$$
$$\iint d^2R\,\nabla_\perp\nu_i\bullet L\{\mathbf{V}\}$$

$$\delta W_{11}(\nu_i,U)+\delta W_{12}(\nu_i,\omega)+\delta W_{13}(\nu_i,\chi)$$
$$\delta W_{21}(\nu_i,U)+\delta W_{22}(\nu_i,\omega)+\delta W_{23}(\nu_i,\chi)$$
$$\delta W_{31}(\nu_i,U)+\delta W_{32}(\nu_i,\omega)+\delta W_{33}(\nu_i,\chi)$$

same functions!

these “energy terms” add to mass matrix to make a fully stable implicit system.

The sparse matrix equation to be solved for the velocity variables take the form:

$$\begin{bmatrix} S^{\nu}_{11} & S^{\nu}_{12} & S^{\nu}_{13} \\ S^{\nu}_{21} & S^{\nu}_{22} & S^{\nu}_{23} \\ S^{\nu}_{31} & S^{\nu}_{32} & S^{\nu}_{33} \end{bmatrix} \bullet \begin{bmatrix} U \\ \omega \\ \chi \end{bmatrix}^{n+1} = \begin{bmatrix} D^{\nu}_{11} & D^{\nu}_{12} & D^{\nu}_{13} \\ D^{\nu}_{21} & D^{\nu}_{22} & D^{\nu}_{23} \\ D^{\nu}_{31} & D^{\nu}_{32} & D^{\nu}_{33} \end{bmatrix} \bullet \begin{bmatrix} U \\ \omega \\ \chi \end{bmatrix}^{n} + \begin{bmatrix} R^{\nu}_{11} & R^{\nu}_{12} & R^{\nu}_{13} \\ R^{\nu}_{21} & R^{\nu}_{22} & R^{\nu}_{23} \\ R^{\nu}_{31} & R^{\nu}_{32} & R^{\nu}_{33} \end{bmatrix} \bullet \begin{bmatrix} \psi \\ f \\ F \end{bmatrix}^{n+1/2}$$

$$S^{\nu}_{11} = D^{\nu}_{11} = \rho(\nu_i, U) - (\theta \delta t)^2 \delta W_{11}(\nu_i, U)$$

etc.

S^{ν} matrix is self-adjoint!

- Corresponds to projections of the operator equation derived on earlier vg:

$$\left\{\rho - \theta^2 (\delta t)^2 L\right\} \mathbf{V}^{n+1} = \left\{\rho - \theta^2 (\delta t)^2 L\right\} \mathbf{V}^{n} + \delta t \left\{ -\nabla p + \frac{1}{\mu_0} (\nabla \times \mathbf{B}) \times \mathbf{B} \right\}^{n+1/2}$$

- Also contains 2 non-trivial sub-systems (reduced MHD) that conserve appropriate “energy” and are numerically stable

$$\left[S^{\nu}_{11}\right] \bullet \left[U\right]^{n+1} = \left[D^{\nu}_{11}\right] \bullet \left[U\right]^{n} + \left[R^{\nu}_{11}\right] \bullet \left[\psi\right]^{n} \qquad \text{etc.}$$

First 3 δW_{ij} terms

$$\delta W_{11}(\nu_i,U) = +\frac{1}{R^2}\left([U,\psi],[\hat{v}_i,\psi]\right)-\frac{1}{R^2}\Delta^*\psi\left[\hat{v}_i,[U,\psi]\right]-\frac{2F}{R^2}\left[U,\frac{F}{R^2}\right]\hat{v}_{iZ}$$

$$+\frac{F}{R^4}\left(U',[\hat{v}_i,\psi]\right)-\frac{F}{R^4}\left([U,\psi],\hat{v}_i\right)'-\Delta^*\psi\left(\frac{F}{R^4}[\hat{v}_i,U]\right)'-\frac{F}{R^4}\left(\frac{F}{R^2}(U',\hat{v}_i)\right)'$$

$$\delta W_{12}(\nu_i,\omega) = -\frac{2F}{R^2}[\omega,\psi]\hat{v}_{iZ}-\frac{\omega'}{R^2}\left(\psi,[\hat{v}_i,\psi]\right)+\frac{\omega'}{R^2}\Delta^*\psi[\hat{v}_i,\psi]+\frac{F}{R^4}\left(\omega'(\psi,\hat{v}_i)\right)'$$

$$\delta W_{13}(\nu_i,\chi) = -\frac{1}{R^2}\left((\chi,\psi),[\hat{v}_i,\psi]\right)+\frac{1}{R^2}\Delta^*\psi\left[\hat{v}_i,(\chi,\psi)\right]+\frac{2F}{R^2}\hat{v}_{iZ}\nabla\bullet\frac{F}{R^2}\nabla_\perp$$

$$-\frac{F}{R^2}\left[[\hat{v}_i,\psi],\chi'\right]+\frac{F}{R^4}\left((\chi,\psi),\hat{v}_i\right)'-\frac{1}{R^2}\Delta^*\psi\left(\frac{F}{R^2}(\chi,\hat{v}_i)\right)'-\frac{F}{R^4}\left(F[\chi,\hat{v}_i]\right)''$$

-present in 2D

-3D only

$$[a,b]\equiv\left[\nabla a\times\nabla b\bullet\nabla\varphi\right]=\frac{1}{R}\left(a_Z b_R-a_R b_Z\right)$$

$$(a,b)\equiv\nabla a\bullet\nabla b=a_R b_R+a_Z b_Z$$

$$f'\equiv\partial f/\partial\varphi$$

note: at most second order derivatives on each scalar → compatible with C^1 elements

Adaptive Meshing

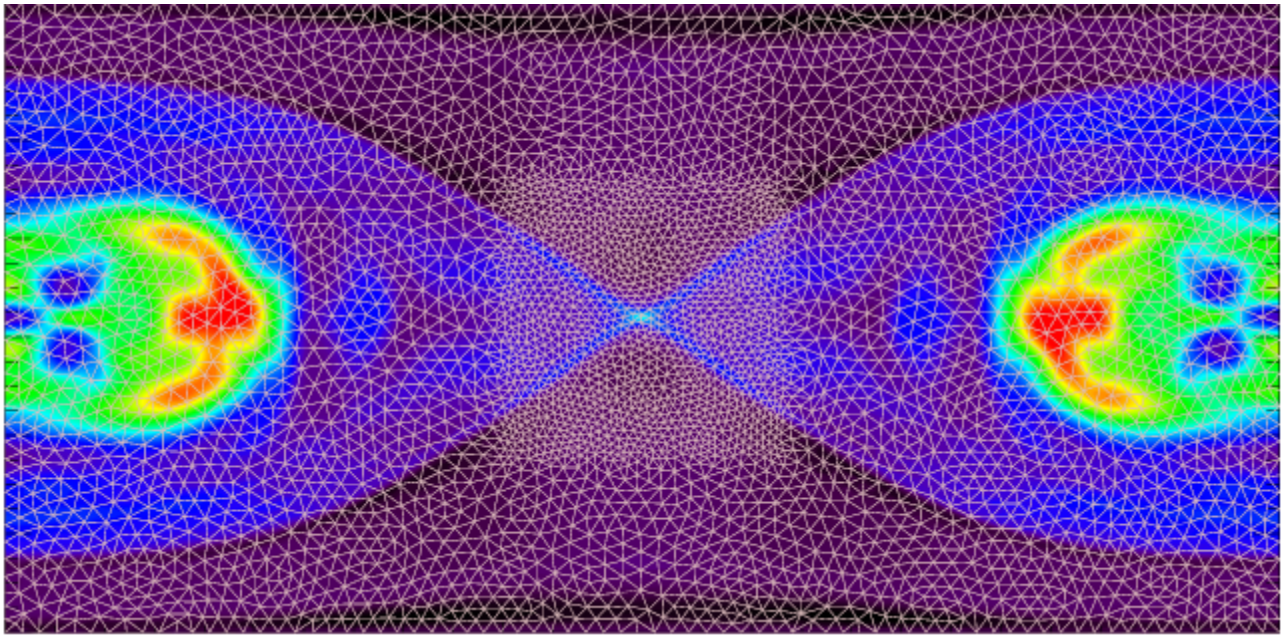

Andy Bauer and the SCOREC center (RPI) have implemented an arbitrary unstructured mesh in the M3D-C^1 code and are exploring different adaptive strategies. This greatly improves the efficiency of the 2-fluid reconnection problem.

SCOREC Routines are now being developed to allow adaptive meshing in arbitrary shaped domains

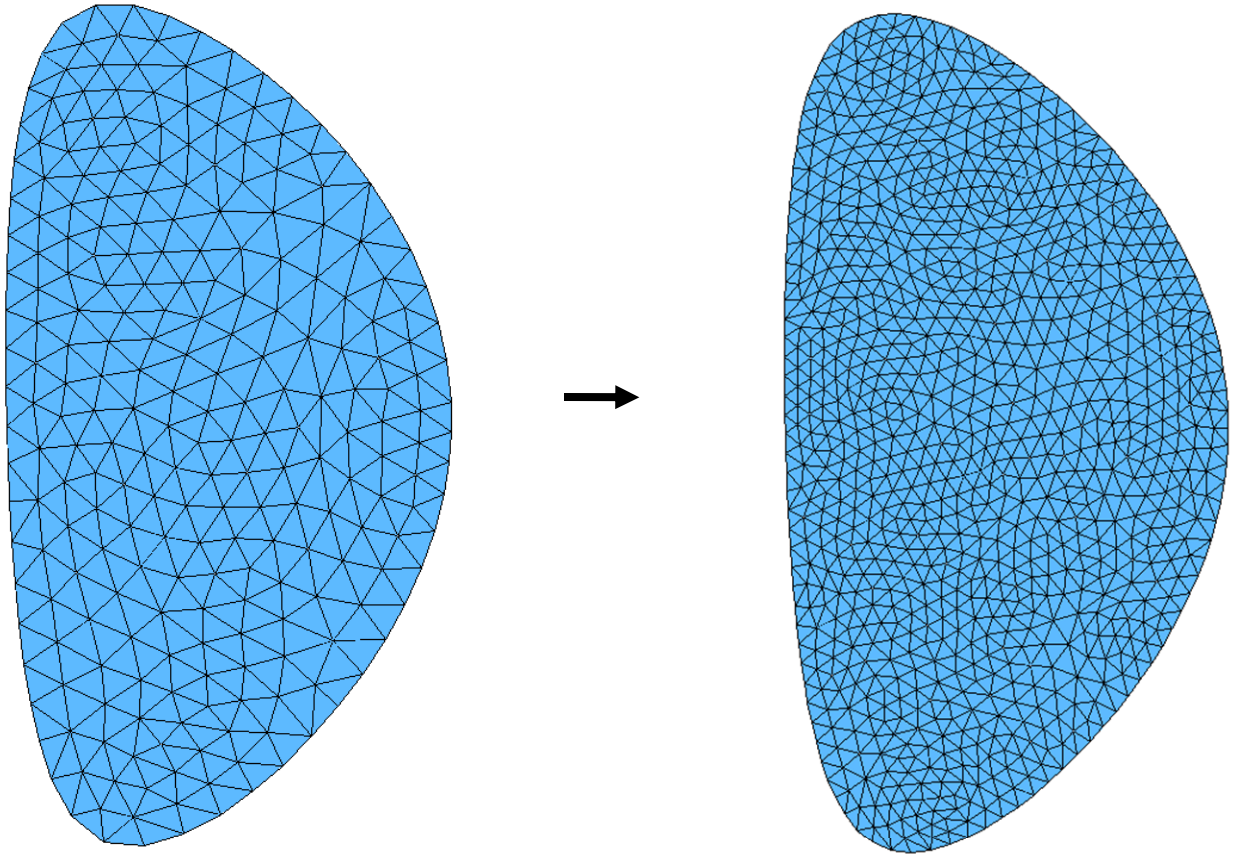

Status and Plans

2D Slab	8-field	• published in JCP (2007) • extended to unstructured, numerical integration • now being applied to guide field reconnection
2D Torus	8-field	• Ferraro thesis (presented at APS 2007) • Steady states with flow to initialize 3D
3D linear	2-field	• RPI group has completed complex software • N. Ferraro has coded and tested • Jessica B. doing physics studies • Now adding resistive wall physics ?
	4-field	• matrix elements derived • intermediate step for debugging
	8-field	• matrix elements derived • will be MARS++ (in time for IAEA?)
3D nonlinear	2-field	• RPI group working on software for 3D time advance—uses PETSC preconditioner options • matrix elements derived
	4-field	• equations shown to conserve energy • intermediate step for debugging
	8-field	• initial results in FY08 ?

In 2D, Implicit equations are solved using either SuperLU_Dist or a PETSc iterative solver

Details for SuperLU-DIST on bassi.nersc.gov:

Mesh points	180 x 180
Matrix Rank	5.9×10^5
# Non-zeros	9.5×10^7
# NZ in L/U	8.8×10^8

# processors	8	32	128
Factor (s)	69.5	38.1	16.9
Gflop/s	27.2	50.1	112.8*

Total problem time (8 processors) for typical high resolution reconnection problem = 208 s x 400 cycles x 8p = 185 p-hrs

Note that for linear problem, Matrix need only be factored once. For semi-implicit method, matrix needs to be factored only occasionally.

*NOTE: In 3D, if we had 100 planes with simultaneous instances of SuperLU, this would be 12,800 p and 11.2 Tflop/s actual!

Summary and Conclusions

- M3D-C^1 approach with Q_{18} elements and stream function/potential form of vector fields has been demonstrated in 2D slab geometry
- Split-Implicit time advance shown to be efficient and stable method for non-trivial problems..close relation to ideal MHD δW
- Full system of equations contains 2 subsets of reduced MHD
- 2-fluid reconnection problems require hyper-resistivity and localized regions with high resolution…natural for adaptive refinement
- When guide field is added, 2F reconnection rate decreases. Resistivity does not play a role in non-linear reconnection. This implies that the $S^{-1/2}$ scale does not need to be resolved in modeling high temperature fusion devices.
- 2D code has been generalized to toroidal geometry for study of spontaneous rotation in tokamaks (Ferraro)
- 3D linear extension is in hand. Initial results for 2-variable reduced MHD (Jessica B.)
- 3D nonlinear extensions underway